AMERICAN JOURNAL OF ENVIRONMENT AND CLIMATE (AJEC)

ISSN: 2832-403X (ONLINE)

VOLUME 2 ISSUE 1 (2023)

PUBLISHED BY

E-PALLI PUBLISHERS, DELAWARE, USA

American Journal of Environment and Climate (AJEC)

Volume 2 Issue 1, Year 2023
ISSN: 2832-403X (Online)
DOI: https://doi.org/10.54536/ajec.v2i1.1188
https://journals.e-palli.com/home/index.php/ajec

Modeling of Hydrodynamic Dispersion in the Sidi Kirayr Locality's Coastal Unconfined Aquifer West of Alexandria, Egypt

Mohamed M. M. Amin[1], Medhat M. H. ElZahar[1*]

Article Information

Received: January 08, 2023
Accepted: March 02, 2023
Published: March 11, 2023

Keywords

Coastal Area, Dispersion, Dispersion Co-efficient, Hydrodynamic Dispersion, Salt Concentration

ABSTRACT

The finite difference method was used in this study to solve the two-dimensional hydrodynamic dispersion equation for a typical coastal unconfined aquifer. A mathematical model is prepared to solve this dispersion problem, which is then modeled and analyzed over time. The salinity profiles for the aquifer transition zone in the Sidi Kirayr locality are determined using the finite difference method. The computed salinity profiles are compared to those obtained from an actual well drilled in the area and used to determine electric conductivity. Profile correlation reveals a roughly parallel trend along the tested depth interval. Additionally, these results correlate well with the chemical analysis of water from the same well. The current work promotes the application of the solution methodology in comparable coastal regions in the absence of dispersion measures for the analyzed aquifer. This innovative approach can be used to forecast groundwater quality in comparable coastal regions. It can also help in selecting the ideal sites for man-made wells that pump groundwater.

INTRODUCTION

Many of us think of lakes, rivers, and streams as sources of water, in other words, surface water. However, approximately 97% of the world's usable freshwater is groundwater. According to the UN, underground storage of 10 million cubic kilometers of water exists. According to the United States Geological Survey, there are approximately 4.2 million cubic kilometers of water within 0.8 kilometers of the earth's surface. Because of the distance between the northwestern coastal line and the Nile River, Egypt's northwestern coastal zone requires novel approaches to water conservation. The study of the quality of groundwater and its suitability for human use is an important environmental issue. Because of the long distance between these areas and the Nile River, Egypt's main source of fresh water, studying the quality of groundwater in coastal areas is an important issue. This study used the finite difference method and a computer program to solve the two-dimensional hydrodynamic dispersion equation with time for a typical coastal unconfined aquifer.

The finite difference method is used to detect salinity profiles for the aquifer's transition zone in the Sidi Kirayr locality. The computed salinity profiles are compared to those obtained from an actual well drilled in the area and used to measure electric conductivity. The correlation of profiles shows a nearly parallel trend along the tested depth interval. These findings are also consistent with the chemical analysis of water from the same well, indicating good agreement. The study promotes the application of the mathematical approach in comparable coastal regions in the absence of dispersion measurements for the studied aquifer. This can be used to forecast the water quality in nearby coastal regions. It can also help in selecting the ideal sites for man-made wells that pump groundwater.

When a freshwater coastal aquifer is discharged into the sea, fresh and saline water meet, and a transition zone is formed between the two types of water. Although the freshwater is lighter than the saltwater, a mixing of saltwater and freshwater occurs. However, the interface formed between the fresh and the underlying saltwater is not sharp but is represented by a mixing zone. The salinity of this zone varies from that of freshwater to that of seawater downwards.

Hydrodynamic dispersion in unconfined aquifers has been a problem in groundwater exploitation and utilization in many coastal aquifers in Egypt's northwestern coastal zone, such as the coastal unconfined freshwater aquifer in the Sidi Kirayr locality, 32 kilometers west of the city of Alexandria, Figure 1. However, the hydrodynamic dispersion problem will be studied in greater detail here.

Solutions to the problems of dispersion in porous media have been obtained by many investigators, (Hunt, 1973; Hunt, 1978; Mariño, 1978; Basak and Murty, 1977; Basak and Murty, 1978; Singh and Murty, 1980; Fattah and Hoopes, 1985; List *et al.*, 1990; Hondzo *et al.*, 1991). Common to these is the solution of the dispersion equation of the typical unconfined aquifer of the Sidi Kirayr locality. (Somaida, 1993), has applied the finite difference method for a preliminary solution of the dispersion equation for the unconfined aquifer in the same locality. The problem has been modeled and investigated. These models, (Somaida, 1993) are tested, and the results of salinity depth profiles are deficient in the qualitative and quantitative interpretation of the salinity profiles.

In previous research papers, the numerical groundwater modeling approach has discussed the significance of groundwater as a significant source of freshwater. It is used to quantify spatial and temporal trends in groundwater flow and availability as well as to examine

[1] Department of Civil Engineering, Faculty of Engineering, Port Said University, Port Fouad 42523, Port Said, Egypt
[*] Corresponding author's e-mail: medhat.alzahar@eng.psu.edu.eg

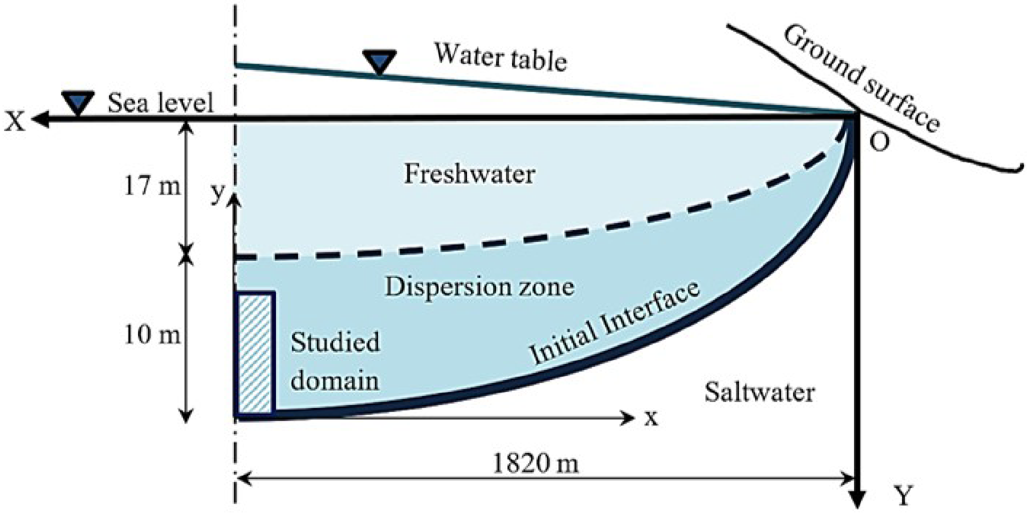

Figure 1: Definition sketch for the studied coastal unconfined aquifer

the overall effects of human activity, (Abdalla, 2016; Al-Dabbas, 2020; Imagawa *et al.*, 2012; Matić and Srzić, 2021).

The present study will concentrate on promising models, where their results will be compared with the real data encountered in the area. The present study will be conducted on two concepts. First, the two-dimensional dispersion equation is derived as applied to a typical unconfined coastal aquifer. Second, numerical computation of the studied aquifer's dispersion equation to reach the vertical groundwater zonation based on aquifer vertical water quality measurements. The water quality results as indicated by electrical conductivity measurements are assured by comparison with the vertical geochemistry zonation performed at the same aquifer.

Mathematical and numerical modeling can help in solving many engineering problems and that can save time and effort (Amin and ElZahar, 2022, Sharaan *et al.*, 2022; Somaida *et al.* 2011, ElZahar *et al.*, 2001; Fujisaki and ElZahar, 2002).

MATERIALS AND METHODS

Finite Difference Formulation

The general differential equation for the distribution of dissolved salts in groundwater under unsteady state conditions in a porous medium is, (Anon, 1965)

$$\frac{\partial}{\partial x}\left(D_x\frac{\partial c}{\partial x}\right)+\frac{\partial}{\partial y}\left(D_y\frac{\partial c}{\partial y}\right)+\frac{\partial}{\partial z}\left(D_z\frac{\partial c}{\partial z}\right)$$
$$-\left(\frac{\partial}{\partial x}(V_x\, c)+\frac{\partial}{\partial y}\left(V_y\, c\right)+\frac{\partial}{\partial z}(V_z\, c)\right)=\frac{\partial c}{\partial t} \quad (1)$$

Where c = concentration of the salt in groundwater, Dx, Dy, and Dz = the dispersion coefficients, Vx, Vy, and Vz = the average pore velocities in the directions (x, y, z), and t = time. The first term on the left-hand side of (Eq. 1) depicts the diffusional transport and the second group, the convectional transport.

Considering a two-dimensional problem, (Eq. 1) can be

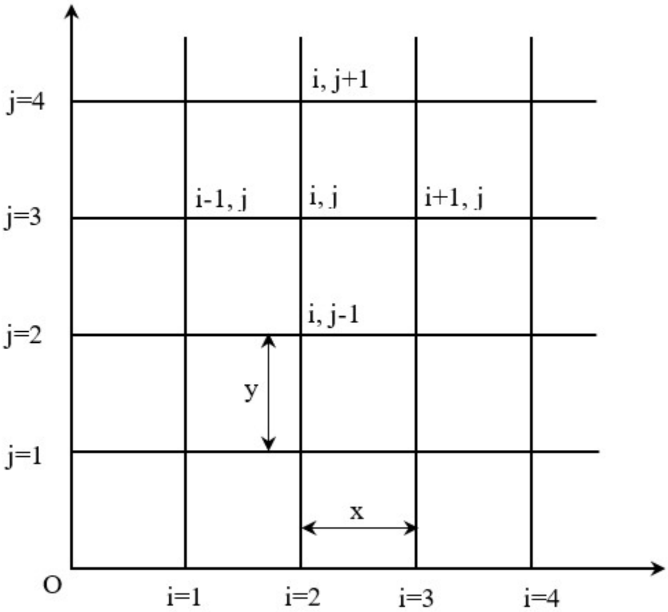

Figure 2: Rectangular mesh for the application of the finite difference technique

simplified to:

$$D_x \frac{\partial^2 c}{\partial x^2} + D_y \frac{\partial^2 c}{\partial y^2} - V_x \frac{\partial c}{\partial x} - V_y \frac{\partial c}{\partial y} = \frac{\partial c}{\partial t} \quad (2)$$

Equation (2) is a second-order differential equation that can be rewritten in the following form:

$$D_{xx}\, c_{xx} + D_{yy}\, c_{yy} - V_x\, c_x - V_y\, c_y = c_t \quad (3)$$

Where,

$$c_{xx} = \frac{\partial^2 c}{\partial x^2},\ c_{yy} = \frac{\partial^2 c}{\partial y^2},\ c_x = \frac{\partial c}{\partial x},\ c_y = \frac{\partial c}{\partial y} \text{ and } c_t = \frac{\partial c}{\partial t}.$$

It is noted here that the changes in Dx and Dy are negligible. In this problem, the concentrations can be known along any boundary, hence, it will be a boundary value problem.

A classical method for numerically approximating a solution for a boundary value problem for this type of equation consists of replacing each derivative in the differential equation with a difference quotient that approximates the derivative, (McCormik and Salvadori, 1968; Wagle and Saff 1986), then:

$$(c_{xx})_{i,j} = \frac{1}{(\Delta x)^2} + \left(c_{i+1,j} - 2\, c_{i,j} + c_{i-1,j}\right) \quad (4)$$

$$(c_{yy})_{i,j} = \frac{1}{(\Delta y)^2} + \left(c_{i,j+1} - 2\, c_{i,j} + c_{i,j-1}\right) \quad (5)$$

$$(c_x)_{i,j} = \frac{1}{2\,\Delta x}\left(c_{i+1,j} - c_{i-1,j}\right) \quad (6)$$

$$(c_y)_{i,j} = \frac{1}{2\,\Delta y}\left(c_{i,j+1} - c_{i,j-1}\right) \quad (7)$$

$$(c_t)_{i,j} = \frac{1}{\Delta t}\left(c_{i,j+1} - c_{i,j}\right) \quad (8)$$

Where Δx = the spacing in the x-direction and Δy = the spacing in the y-direction, (Figure 1,) and Δt = the time step.

$$\left(\frac{1}{\Delta t} + \frac{(V_y)_{i,j}}{2\Delta y} - \frac{D_y}{(\Delta y)^2}\right) c_{i+1,j} = \left(\frac{D_x}{(\Delta x)^2} - \frac{(V_x)_{i,j}}{2\Delta x}\right) c_{i,j+1} + \left(\frac{D_x}{(\Delta x)^2} + \frac{(V_x)_{i,j}}{2\Delta x}\right) c_{i,j-1} + \left(\frac{D_y}{(\Delta y)^2} + \frac{(V_y)_{i,j}}{2\Delta y}\right) c_{i-1,j} + \left(\frac{1}{\Delta t} - \frac{2D_x}{(\Delta x)^2} - \frac{2D_y}{(\Delta y)^2}\right) c_{ij} \quad (9)$$

However, if it is assumed that the dispersion coefficient, D, does not change with time or distance in porous medium and taking equal spacings in the directions X and Y (Δx = Δy = Δ), then (Eq. 9) is simplified to:

$$\left(\frac{1}{\Delta t} + \frac{(V_y)_{i,j}}{2\Delta} - \frac{D}{(\Delta)^2}\right) c_{i+1,j} = \left(\frac{D}{(\Delta)^2} - \frac{(V_x)_{i,j}}{2\Delta}\right) c_{i,j+1} + \left(\frac{D}{(\Delta)^2} + \frac{(V_x)_{i,j}}{2\Delta}\right) c_{i,j-1} + \left(\frac{D}{(\Delta)^2} + \frac{(V_y)_{i,j}}{2\Delta}\right) c_{i-1,j} + \left(\frac{1}{\Delta t} - \frac{4D}{(\Delta)^2}\right) c_{ij} \quad (10)$$

(Eq. 10), can be used to determine the concentration C at any pivotal point in the flow domain and is derived according to the following assumptions.

1) One phase flow, the aqueous phase consists of two components water and salt. 2) Fluid is incompressible. 3) Homogeneous, isotropic porous medium with constant dispersion coefficient. 4) Two-dimensionalnal unsteady flow in the porous medium .

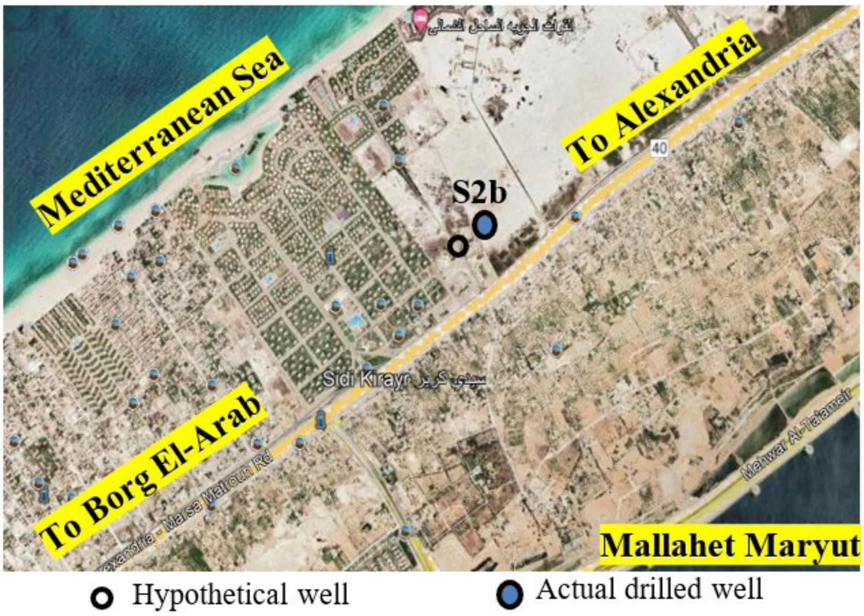

Figure 3: Volume of trash cans

Determination of Parameters

This can be done through the application of the finite difference method on the actual condition of the coastal unconfined aquifer of the Sidi Kirayr locality west of Alexandria, (Abdel-Mogeeth and Elshazly, 1980), Figure 3. In this aquifer the water table is determined according to measurements of groundwater levels in the native wells scattered in the area and the fresh-saltwater interface is determined theoretically by Ghyben-Herzberg principle and practically by meaning the electrical conductivity in certain test wells in the area (Abdel-Mogeeth and Elshazly, 1980). A typical vertical cross-section of the studied aquifer is shown in Figure 4. The studied aquifer zone is selected along the center line of the aquifer (location of the hypothetical well, Figure 3) through the dispersion zone formed between fresh and saltwater. The salinity profile along this line, Figure 5, shows an abrupt change of salinity from 2 mmhos to about 39 mmhos at depths from 24-28 m.

However, the dispersion zone in the lower 10 meters (28 to 38 m), is considered to be detected and analyzed, where the salinity changes gradually from 39 to more than

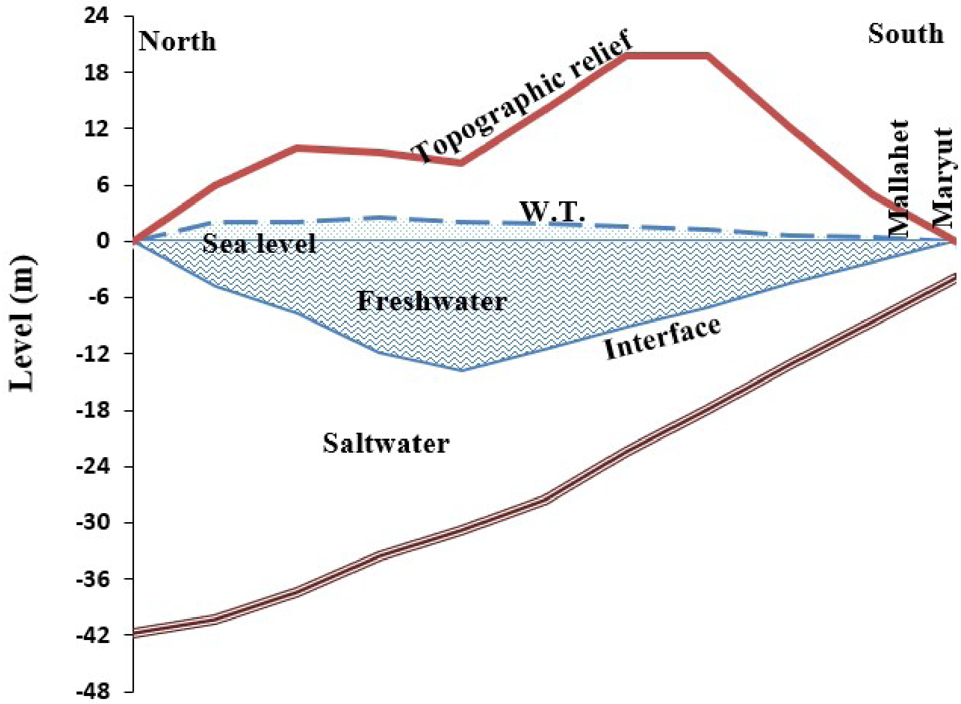

Figure 4: Extent of fresh and saltwater in the Sidi Kirayr coastal unconfined aquifer, northwestern coastal zone, Egypt (Somaida, 1993)

50 mmhos. The selected domain is a rectangular mesh, 10 m in length and 4 m in width.

Concentrations are given along the left boundaries, while those at the right one are to be computed.

The average hydraulic conductivity of the aquifer K = 10 m/day, the effective porosity n = 0.2, and the average upward pore velocity Vy = 0.05 m/day, determined from the study of water table levels in the area and the use of Ghyben-Herzberg principle, (Somaida, 2014; Wirojanagud and Charbeneau, 1985).

The average pore velocity in the X-direction Vx is dete… omain using the follo…

$$(V_x)_{i,j} = \frac{(d_s - d_f)\, K\, Y_{i,j}}{2\, n\, X_{i,j}} \qquad (11)$$

where ds and df are specific gravities of the sea and freshwater (l.025, 1.0), and X and Y are the coordinates of the pivotal point from the origin which is taken as the location of the hypothetical well, Figure 3.

The dispersion coefficient can be calculated using the following equations and the field data as follows:

For transition zone length, (Schmork and Mercado, 1969):

$L_{mix} = Z_{(c=0.159)} - Z_{(c=0.841)}$ (12)

Where,

Zc=0.159 = depth relative to 0.159 of the initial concentration and Zc=0.841 will be relative to 0.841.

From Figure 5, it is found 11.6 m.

The mixing length as a function of Zrise (interface rise) and dispersivity a1, is given by:

$L_{mix} = 2\sqrt{(2\, a_1\, Z_{rise})}$ (13)

The decline of the water table in the actual well S2b, Figure 3, is 0.125, then according to Herzberg principle, Z_{rise}=40*0.12=4.8 m. However, the application of Eq. 13 gives 11.6=2 $\sqrt{(2\, a_1 * 4.8)}$, then dispersivity of the aquifer = 3.5 m.

According to Ref (18), the dispersion coefficient varies approximately directly with Vx. The ratio D_L/Vx, theoretically is a constant, called the dispersivity having the dimension of length and in the present study = 3.5=D_L/V_x . Here Vx is calculated as equal to KI, where K = hydraulic conductivity of the aquifer = 10 m/day and I is the hydraulic gradient in the transverse direction at nearly the middle of the asphalt road (location of htheypothetical well) = 0.125/46.7=0.0027.

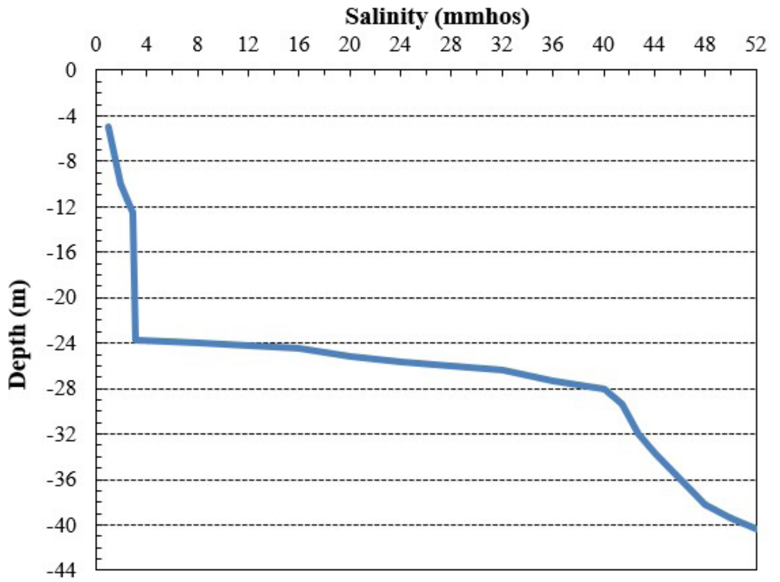

Figure 5: Observed water salinity with depth at the center of the studied aquifer (Somaida, 1993)

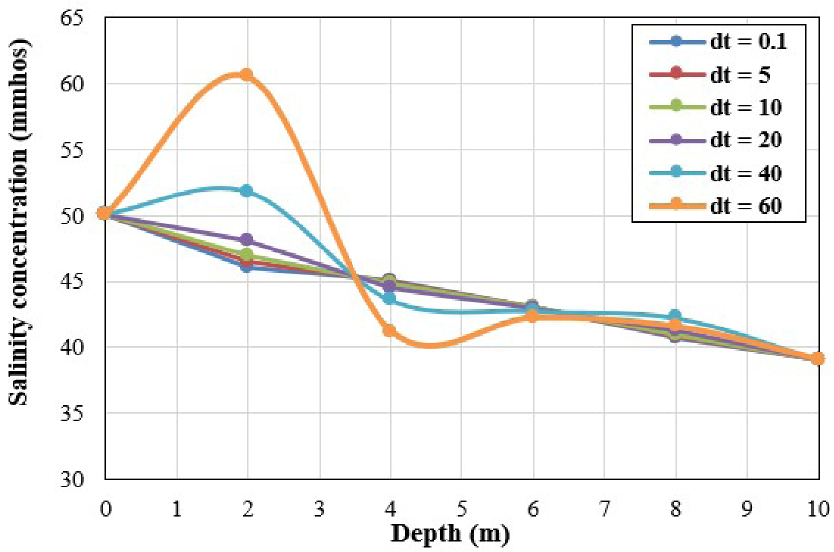

Figure 6. a: Concentration results and their graphical representation along the studied profile (Model M1)

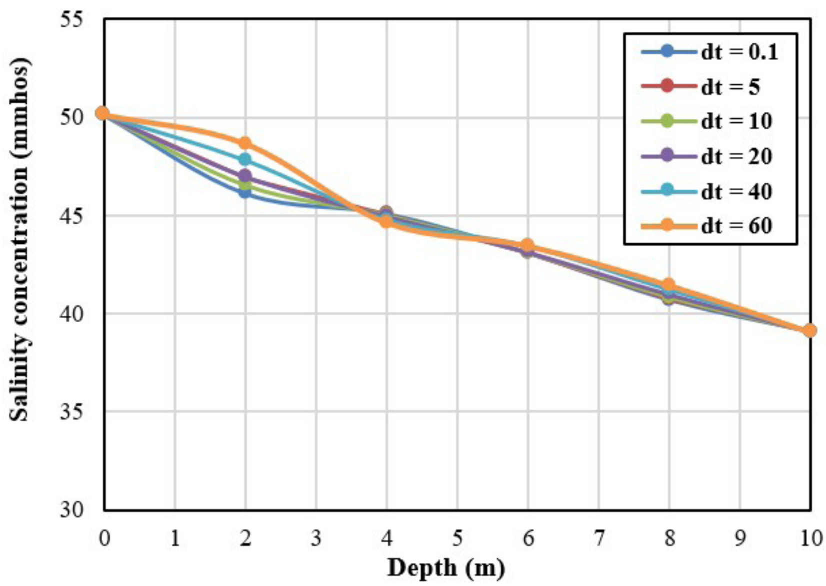

Figure 6. b: Concentration results and their graphical representation along the studied profile (Model M2)

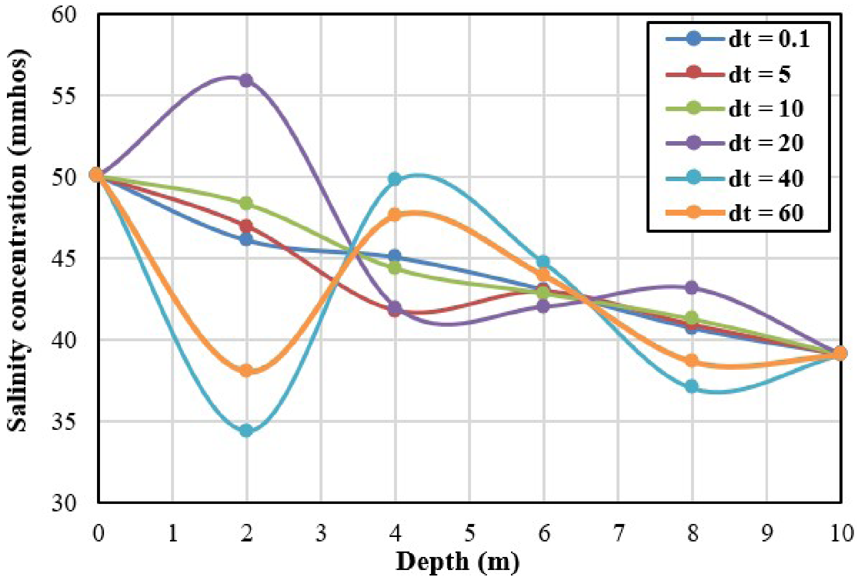

Figure 6. c: Concentration results and their graphical representation along the studied profile (Model M3)

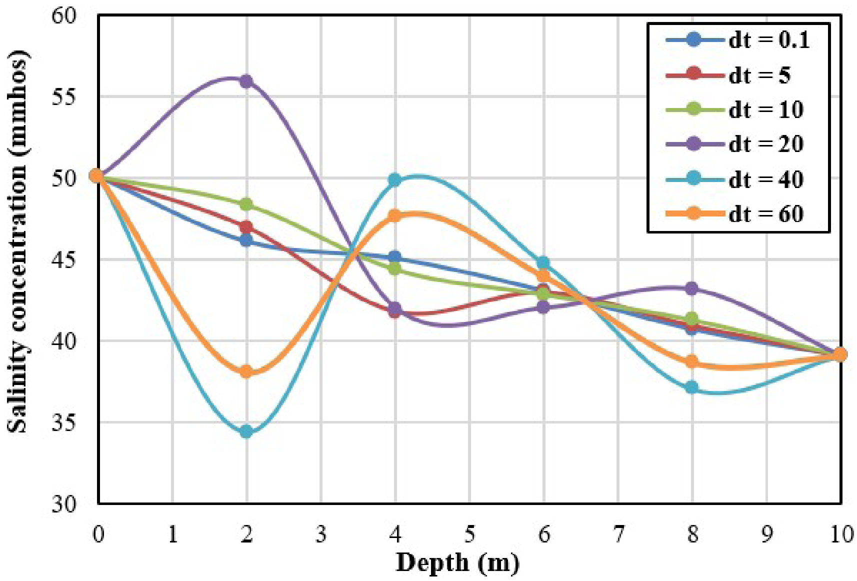

Figure 6. c: Concentration results and their graphical representation along the studied profile (Model M3)

However, V_x=10*0.0027=0.027 m/day, from which, D_L=3.5*0.027=0.095 m^2/day.

Numerical Study

A computer program for the solution of the dispersion expression, Eq. 10, is developed. The program required the knowledge of the concentrations at the left side of the proposed domain together with distance step Δ, time increment Δt and the diffusion coefficients D. In this view, six mathematical models are employed (M1 to M6). For M1, M2 and M3, the increment, Δ is taken 2 m and dispersion coefficients of 0.095, 0.0475, and 0.19 m^2/day, respectively. The same choice is decided for M4, M5, and M6.

• Model M1, Figure 6-a, shows satisfactory concentration values with depths which are close to the values measured in the field until Δt=20 days. At time t = 40 days, concentrations are nearer to the real values in the upper and lower 4 meters in the studied aquifer. While at t = 60 days, the concentrations are highly oscillating and far from the real values.

• Model M2, Figure 6-b, shows satisfactory trends but the concentrations are less than the expected values.

• In model M3, Figure 6-c, the concentrations are mostly far from the actual values. High oscillations are very evident along the salinity profile.

• Models M4, M5, and M6, Figs. 6-(d-f), indicated bad plots which are completely out of phase, indicating the lack of a general trend for salinity.

However, it is discovered from the studied models that the best values of the aquifer's dispersion coefficient D

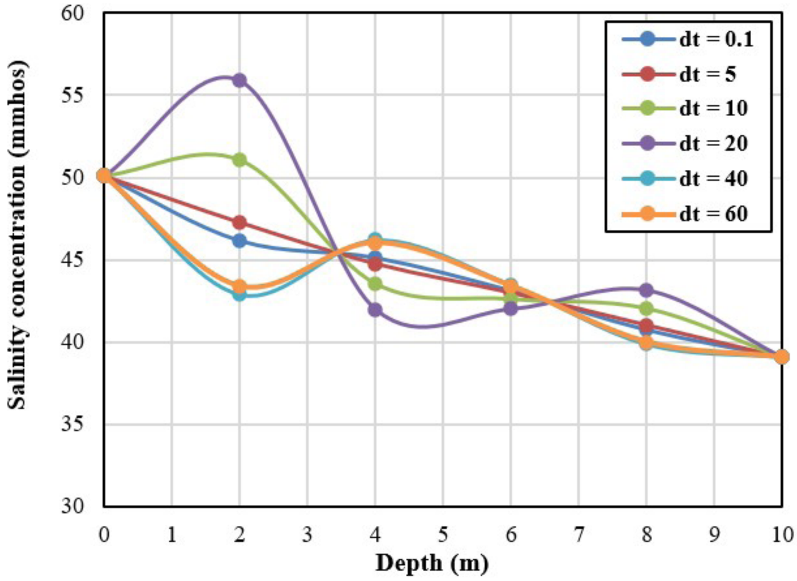

Figure 6. d: Concentration results and their graphical representation along the studied profile (Model M4)

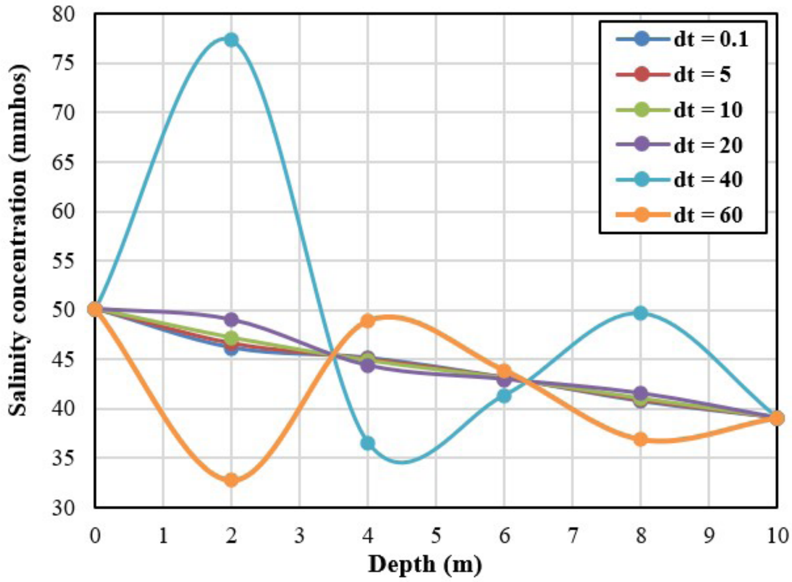

Figure 6. e: Concentration results and their graphical representation along the studied profile (Model M5)

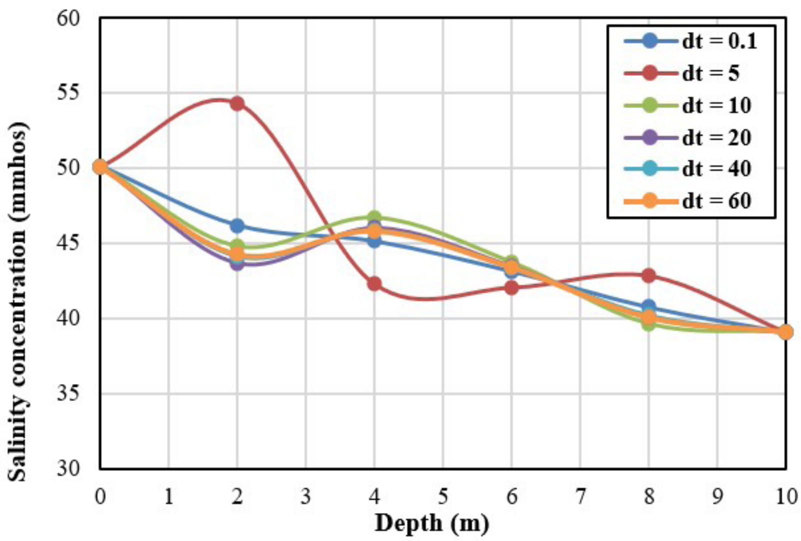

Figure 6. f: Concentration results and their graphical representation along the studied profile (Model M6)

are 0.095 m2/day. The best and most trustworthy results for further research in this paper come from model M1.

RESULTS AND DISCUSSION

Hydrodynamic dispersion in the coastal aquifer

It appears that the longitudinal dispersion of fresh and saltwater is active upward in coastal unconfined aquifers as explained by (Anon, 1965). Since in coastal aquifers, fresh water will be contaminated from saline water and the concentration of fresh water will be increased with increasing distance of flow upward because of hydrodynamic dispersion, longitudinal dispersion occurs in the direction of flow and is caused by different macroscopic velocities as some parts of the salt invading water move through wider and less tortuous pores than other parts, (Bouwer, 1985). The different rates of advance produce the typical sigmoid breakthrough curves of the invading saline water at the same distance from the front of the invading fluid. This phenomenon is best developed in the coastal aquifer of the Sidi Kirayr area and is observed in the detecting the test well S2b, in the Sidi Kirayr locality, Figure 3, which is drilled to a depth of 38 m, the depth of water table = 10 m. The well is completely penetrating the aquifer and its discharge is about 60 m^3/day (6.94 * 10^{-4} m^3/sec), Figure 5.

Table 1: Distribution of households surveyed by neighborhood, type, number, and size

Depth (m)	36	32	28	24	20	18	16	12	8
Detected EC mmhos, S2b	54.9	48.1	42.6	17.15	12.86	2.75	2.46	2.3	2.2
Computed EC mmhos, M1			50.1	44.5	41.2	19			
Computed EC mmhos, M2			50.1	44	41	39			

Computed concentration-depth profiles for the studied aquifer

Table 1 depicts the profiles from which the concentration-depth profiles are constructed, as well as the models M1 and M2, Figure 5, and the real concentration-depth profile associated with the actual well S2b, Figure 7. Investigation of this figure leads to the following conclusions:

- Concentration (salinity) increases with depth.
- Both profiles, the real and M1, have the same trend in which the relatively sigmoid breakthrough curves are observed.
- The profile M2 shows oscillating salinity values relative to M1, far from the expected values, which can be safely disregarded.

The M1 profile shows satisfactory results which are nearer to the actual field values. This is attributed to the proper choice of model M1 and its necessary data as; depth increment Δ, time step Δt and the diffusion coefficient D relative to the actual field data from the Sidi Kirayr locality.

Comparison between computed and detected salinity depth profiles

For this purpose, Table 1, showing the variations of concentrations with depth and salinity profiles in Figure 7, is discussed and the following conclusions are reached:

- The salinity profiles show the same trend in the interval from 24-28 m and are nearly parallel profiles. This may indicate the correction of the approach of the derived dispersion Eq. 10, its solution, and assumptions.
- There is a marked decrease in salinities in the actual test well S2b below the computed values. This may be attributed to the nature of the geochemistry of the water in the actual test well S2b.

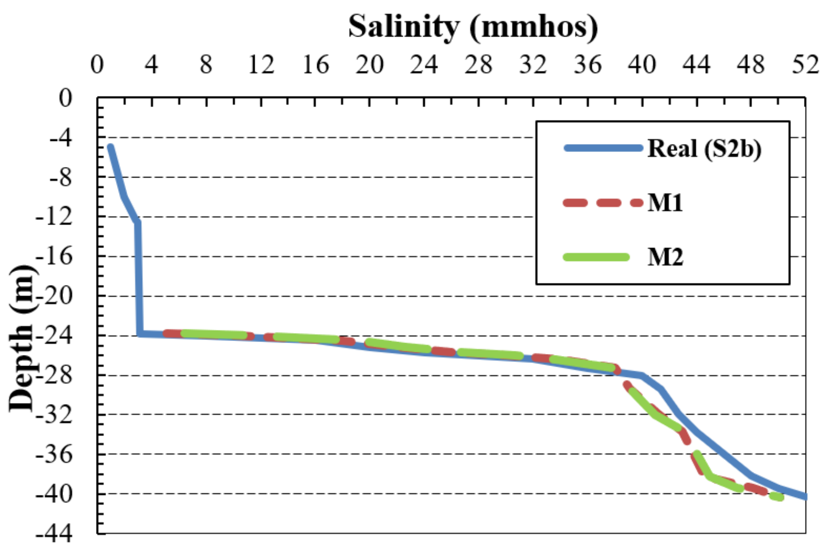

Figure 7. Correlation of salinity profiles; Real (S2b), computed M1, and M2

• In both cases, the rate of salinity change increases with depth, where the actual sea water is found at depth of 38 m, (Anon, 1965).

Vertical Zonation of Groundwater

In coastal aquifers, freshwater is physically defined as water having specific gravity of 1.0, which is floating over

Freshwater	2	Mmhos
Passably freshwater	2-4	Mmhos
Brackish water	4-9	Mmhos
Saltwater	9-50	Mmhos
Extremely saltwater	>50	Mmhos

saltwater of specific gravity of about 1.025. In terms of total salinity, expressed as electrical conductivity/cm at 25 ^{o}C, water is classified as follows, (Matić and Srzić, 2021):

Therefore, the vertical zonation of the freshwater lens in the Sidi Kirayr area has been followed up by using the electrical conductivity meter in the actual well S2b. This well is completely penetrating the aquifer and is fully perforated from top to bottom to give a coherent picture of the water salinity sequence. Such well is drilled down to reach the level of 36 m below the sea level, (Abdel-Mogeeth and Elshazly, 1980).

On the other hand, the projection of salinity value in mmhos of the water classification according to (Hem, 1985), over the salinity profiles, Figure 7, shows that four main water zones are distinguished as shown in Table 2.

Investigation of these zones leads to the following classification:

• A zone of passably freshwater class<4 mmhos or (2-4) of depth 8-20.6 m, in well S2b. The corresponding change in salinity is 0.16 mmhos/m.

• A zone of brackish water (4-9 mmhos), from 20.6 to 27 m. This zone has a thickness of 1.4 m, however, it will not be important.

• A zone of salt water (9-50 mmhos) from (22-36 m) is evident in real well S2b and may be from (14.8-28 m) in salinity profile M1. The latter indicated that saltwater appears at a shallow depth of 14.8 m and goes to 22 m in well S2b.

• It is noted that in Figure 7, the transition zone of width 2b = 11.6 m in the depth range from 22-39.8 m, i.e., lies in the saltwater zone.

Although the changes in salinity are 2.93 and 3.1 mmhos/m depth in both cases, to avoid any confusion, it

Table 2: Classification of groundwater according to salinity profiles in the Sidi Kirayr are, (Hem 1985)

Freshwater	2	Mmhos
Passably freshwater	2-4	Mmhos
Brackish water	4-9	Mmhos
Saltwater	9-50	Mmhos
Extremely saltwater	>50	Mmhos

is recommended that reliance should be made on the real data obtained from measuring the electrical conductivity in real test well S2b, Figure 3.

CONCLUSIONS

In the present study, the finite difference method has been applied to develop and solve the dispersion equation for a typical unconfined aquifer as the case implies in the Sidi Kirayr locality, west of Alexandria, Egypt, where the problem has been modeled and investigated.

Numerical calculations of the concentration of water with depth in an actual tested well in the area have been reached using a well-developed computer program, which solves the dispersion equation and obtains the water salinity at a depth varying from 18 to 38 m along a computed vertical profile at the center of the lens. In addition, electrical conductivity measurements were performed in the test well S2b, which is very close to the lens' center.

When the computed salinity profile below a good example was compared to the measured salinity profile in well S2b, there was an order of magnitude agreement. The sigmoid breakthrough curves of both situations exhibited nearly parallel trends, indicating that the electrical conductivity measurements were successful. Also, this shows that the vertical zonation of groundwater in the Sidi Kirayr locality can be distinguished into three characteristic water zones: a top fresher water zone (2-4 mmhos), a brackish water zone, then a salt water to seawater zone. Finally, below this, there is the actual seawater of the Mediterranean Sea above 50 mmhos salinity. The latter results are found to be in good agreement with those reached by (Abdel-Mogeeth and Elshazly, 1980).

Nomenclature

C = Concentration,
Δt = Time increment,
Vx = Velocity of flow in the X-direction,
Vy = Velocity of flow in the Y-direction,
Δx = Distance increment,
D = Dispersion coefficient of aquifer,
ds = Specific gravity of saltwater,
df = Specific gravity of freshwater,
K = Hydraulic conductivity of the aquifer,
n = Porosity of the aquifer,
xi,j = Horizontal coordinates of the pivotal point,
yi,j = Vertical coordinates of the pivotal point,
Lmix = Length of transition zone (mixing length),
a1 = Dispersivity,
Zrise = Rise of interface measured from reference level,
DL = Longitudinal dispersion coefficient.

REFERENCES

Abdalla, F. (2015). Ionic ratios as tracers to assess seawater intrusion and to identify salinity sources in Jazan coastal aquifer, Saudi Arabia. *Arabian Journal of Geosciences, 9*(1). https://doi.org/10.1007/s12517-015-2065-3.

Abdel-Mogeeth, S. M., and Elshazly, M.M. (1980). Characteristics of the freshwater lens in Sidi Kirayr locality, North-western coastal zone, Egypt. *Desert Institute Bulletin, A.R.E., 30*(1), 1-15.

Al-Dabbas, M. (2020). Management Of Bai Hassan Unconfined Aquifer, Lesser Zab River Basin, Kurdistan Region, Iraq Using A Modeling Approach. *Iraqi Geological Journal, 53*(2B), 1–23. https://doi.org/10.46717/igj.53.2b.1rs-2020-08-01.

Anon, (1965). International Atomic Energy Agency. Radioactive waste disposal in the ground. AEA, Vienna, STI/PUB/103.

Amin, M. M. M., & ElZahar, M. M. H. (2022). Economic Design Of Pipe-Nozzle Discharge Lines Delivering Free Jets. *International Journal of Engineering Technologies and Management Research, 9*(10), 10–25. https://doi.org/10.29121/ijetmr.v9.i10.2022.1232.

Basak, P., & Murty, V. V. N. (1977). Nonlinear diffusion applied to groundwater contamination problems. *Journal of Hydrology, 35*(3–4), 357–363. https://doi.org/10.1016/0022-1694(77)90012-9.

Basak, P., & Murty, V. V. N. (1978). Concentration-dependent diffusion applied to groundwater contamination problems. *Journal of Hydrology, 37*(3–4), 333–337. https://doi.org/10.1016/0022-1694(78)90024-0.

Bouwer, H., (1978). Groundwater hydrology. New York: McGraw-Hill, 480.

El-Zahar, M., M. Salih, and K. Fujisaki. (2001). Basic study of bubble formation in dissolved CO_2 gas flotation of waste activated sludge. *Proceedings of FILTECH EUROPA International conference and Exhibition, 1*.

Fattah, Q. N., & Hoopes, J. A. (1985). Dispersion in Anisotropic, Homogeneous, Porous Media. *Journal of Hydraulic Engineering, 111*(5), 810–827. https://doi.org/10.1061/(asce)0733-9429(1985)111:5(810).

Fujisaki, K., & El-Zahar, M. (2002). A mathematical model for the flotation of waste activated sludge. *Water Science and Technology, 46*(11–12), 203–208. https://doi.org/10.2166/wst.2002.0739.

Hem, J. D. (1985). Study and interpretation of the chemical characteristics of natural water. Department of the Interior, *US Geological Survey, 2254*. https://doi.org/10.3133/wsp2254.

Hondzo, M., Ellis, C. R., & Stefan, H. G. (1991). Vertical Diffusion in Small Stratified Lake: Data and Error Analysis. *Journal of Hydraulic Engineering, 117*(10), 1352–1369. https://doi.org/10.1061/(asce)0733-9429(1991)117:10(1352).

Hunt, B. W. (1973). Dispersion from Pit in Uniform Seepage. *Journal of the Hydraulics Division, 99*(1), 13–21. https://doi.org/10.1061/jyceaj.0003547.

Hunt, B. (1978). Dispersive Sources in Uniform Ground-Water Flow. *Journal of the Hydraulics Division, 104*(1), 75–85. https://doi.org/10.1061/jyceaj.0004925.

Imagawa, C., Takeuchi, J., Kawachi, T., Chono, S., & Ishida, K. (2012). Statistical analyses and modeling approaches to hydrodynamic characteristics in alluvial aquifer. *Hydrological Processes, 27*(26), 4017–4027. https://doi.org/10.1002/hyp.9538.

List, E. J., Gartrel, G., & Winant, C. D. (1990). Diffusion and Dispersion in Coastal Waters. *Journal of Hydraulic Engineering, 116*(10), 1158–1179. https://doi.org/10.1061/(asce)0733-9429(1990)116:10(1158).

Mariño, M. A. (1974). Longitudinal Dispersion in Saturated Porous Media. *Journal of the Hydraulics Division, 100*(1), 151–157. https://doi.org/10.1061/jyceaj.0003851.

Matić, I., & Srzić, V. (2021). Modeling of seawater intrusion into river Neretva coastal aquifer. *Common Foundations, 2021*. https://doi.org/10.5592/co/zt.2021.12.

McCormik, J. M., and Salvadori, M. G. (1968). Numerical methods in Fortran, Prentice-Hall International, Inc., Engle wood.

Sharaan, M., Lebleb, A. A., ElZahar, M. M. H., & Iskander, M. (2022). Studying the tidal-induced water circulation pattern within EL-Burullus fishing harbor, Egypt, using CMS-PTM numerical modeling. *Marine Environmental Research, 180*, 105726. https://doi.org/10.1016/j.marenvres.2022.105726.

Schmork, S., & Mercado, A. (1969). Upconing of Fresh Water-Sea Water Interface Below Pumping Wells, Field Study. *Water Resources Research, 5*(6), 1290–1311. Portico. https://doi.org/10.1029/wr005i006p01290.

Singh, S. P., & Murty, V. V. N. (1980). Storage of Freshwater in Saline Aquifers. *Journal of the Irrigation and Drainage Division, 106*(2), 93–104. https://doi.org/10.1061/jrcea4.0001304.

Somaida, M. M.(1993). Numerical solution for dispersion in a coastal unconfined aquifer, *Port-Said Scientific Engineering Bulletin, 5*, 280-293.

Somaida, M. M. *et al.* (1980). A study on the flow-net of the freshwater zone in a coastal unconfined aquifer, Numerical solution for dispersion in a coastal unconfined aquifer, Scientific Engineering Bulletin, *Faculty of Engineering, Cairo University, 1*, 21-52.

Somaida, M. M. (2014). Solving the Upconing Pumping Problem and Hydrodynamic Dispersion in Coastal Unconfined Aquifers. *Port-Said Engineering Research Journal, 18*(2), 81–90. https://doi.org/10.21608/pserj.2014.45295.

Somaida, M., Elzahar, M., & Sharaan, M. (2011). A suggestion of optimization process for water pipe networks design. *In International Conference on Environment and BioScience IPCBEE,21,* 68-73.

Wagle, K. R., and Saff, E.B. (1986). Fundamentals of differential equations. Benjamin/Cummings Company Inc., California.

Wirojanagud, P., & Charbeneau, R. J. (1985). Saltwater Upconing in Unconfined Aquifers. *Journal of Hydraulic Engineering, 111*(3), 417–434. https://doi.org/10.1061/(asce)0733-9429(1985)111:3(417).